Preprint Title	Synthesis and characterization of zinc and copper oxide nanoparticles and their antibacterial activity
Authors	Richard B. Asamoah, Abu Yaya, Bismark Mensah, Pascal Nbelayim, Vitus Apalangya, Yaw D. Bensah, Lucas N. W. Damoah, Benjamin Agyei-Tuffour, David Dodoo-Arhin and Ebenezer Annan
Publication Date	22 Jan 2020
Article Type	Full Research Paper
ORCID® iDs	Richard B. Asamoah - https://orcid.org/0000-0003-2508-5533; Pascal Nbelayim - https://orcid.org/0000-0002-2173-0788; Ebenezer Annan - https://orcid.org/0000-0001-8330-0284

Synthesis and characterization of zinc and copper oxide nanoparticles and their antibacteria activity

R. B. Asamoah[1], A. Yaya[1], B. Mensah[1], P. Nbalayim[1], V. Apalangya[2], Y.D Bensah[1], L.N.W. Damoah[1], B. Agei-Tuffour[1], D. Dodoo-Arhin[1], E. Annan[1]*

[1]Department of Materials Science & Engineering, School of Engineering Sciences, CBAS, University of Ghana, Legon, Ghana

[2]Department of Food Process Engineering, Engineering, School of Engineering Sciences, CBAS, University of Ghana, Legon, Ghana

Abstract

Inorganic nano-metal oxides can be effective alternatives to drug resistant organic antibiotics due to their broad spectrum antimicrobial activity against pathogenic and mutagenic gram-negative and positive bacteria. In this study, zinc and copper oxides (ZnO and CuO) were synthesized using a facile wet chemical method. The oxide nanoparticles were characterized using X-ray diffraction (XRD), UV-Vis spectrometer (UV-Vis), Fourier Transformed Infra-red spectrometer and Transmission electron microscopy (TEM). The antibacterial activities of the nanoparticles were investigated against *e. coli* and *s. aureus* using the disk diffusion and microdilution tests. The XRD analysis revealed that both zinc and copper oxide nanoparticles were purely crystalline. The TEM micrographs showed that copper oxide nanoparticles assumed a nanorod shape of average length of 100 nm. Whiles zinc oxide nanoparticles were spherical of average diameter of 15 nm. The FTIR results showed that the nanoparticles were free of impurities and organic surfactants. The optical band gaps of CuO and ZnO according to UV-Vis analysis were respectively 2.63 eV and 3.22 eV. According to the antibacteria tests, the minimum inhibition concentration (MIC) of CuO against *e. coli* and *s. aureus* were correspondingly 1mg/ml and 0.25 mg/ml whiles it was 0.1mg/ml for ZnO against *s. aureus* but ZnO produced no inhibition against *e. coli*. With the microdilution test, both nanoparticles exhibited activity against both bacteria species at all varying concentrations. CuO had an antibacteria efficiency of 80 to 97% and 85 to 99% for *e. coli* and *s. aureus* respectively. The efficiency of ZnO were 20 to 90% and 50 to 89% for *e. coli* and *s. aureus* accordingly. The results concluded that CuO had higher antibacteria activity as compared to ZnO.

Keywords: Antibacteria, nanoparticles, disk diffusion test, optical density test.

Introduction

The incidence of antibiotic resistive pathogens has led to the continuous search for new alternatives (P. K. Pandey *et al.*, 2014). Among drug resistive pathogens, water borne bacteria species pose a real threat to public health as they are responsible for the outbreak of diseases such as diarrhoea which accounts for 2195 global infant mortality per day (CDC, 2018).

Inorganic nanoparticles have demonstrated toxicity against a wide range of pathogenic bacterial species (Kar *et al.,* 2014). Even though, the broad-spectrum biocidal effect of inorganic nanomaterials are well known, the bacteriocidal effect is poorly understood (Franci *et al.*, 2015). It has been proposed that the release of ions into solution creates reactive oxygen species which is toxic to bacteria. Other studies showed that nanoparticles by virtue of their size can penetrate bacterial cell walls and attack organelles which leads to cell death (Foldbjerg *et al.*, 2015). Unlike organic antibiotics, the inorganic counterparts have multi-targeting pathways to combat drug resistive pathogens through mutations (Ivask *et al.*, 2013).

Among inorganic nanoparticles, metal oxide nanoparticles are widely considered for their antibacteria activities (A. Kumar *et al.,* 2013). This is mostly attributed to the fact that metal oxides have easy synthesis routes which can be controlled to tune the size and shape of the nanoparticles and they are also cheaper as compared to metal nanoparticles such as silver and gold (Ahmed *et al.*, 2016). Copper and zinc oxides are considered as suitable alternatives to organic based antimicrobials. Their antibacteria effect is dependent on a number of factors which are mostly determined by the method of synthesis (P. Pandey *et al.*, 2014). These factors include their size, the presence of surfactant, their shape and a host of other factors (Sahooli, Sabbaghi and Saboori, 2012). Metal nanoparticles, due to their small size and high reactivity easily diffuse through the well wall of bacteria to attach themselves to internal proteins and organelles leading to bacteria death (Palza, 2015) (Agnihotri, Mukherji and Mukherji, 2014). The activities of nanoparticles is also affected by the presence of surfactants on their surfaces. Whiles certain surfactants enhance cell growth, others inhibit cell growth and may event cause cell death. The synthesis of nanoparticles with certain surfactant will result in the respective effect of promoting or impeding cell proliferation (Reverberi *et al.*, 2016) For instance, the cationic surfactant; cetyltrimethylammonium bromide (CTAB) is reported to possess antibacteria activity (Nakata, Tsuchido and Matsumura, 2010).The shape of nanoparticles can influences its toxicity (Sahooli, Sabbaghi and Saboori, 2012). Cubic silver nanoparticles were found to be more toxic than its spherical counterpart (Xiu *et al.,* 2012). Among many reasons, this may be chiefly due to their respective release of ionic species in solution which is the major

antibacteria agent. Also, the nanoparticle's diffusive rate through the pores of cell walls (Feng *et al.*, 2000). The permeability of nanoparticles through cell walls is related to the particle size and shape (Chandraker *et al.*, 2015). Therefore, these physical properties of nanoparticles dictate their characteristics which affect their application including antibacteria use. In particular, the antibacteria application is highly reliant upon the ability of the nanoparticle to release ions into solution. Also, its ability to pass through cellular pores to disrupt organelles (El-Trass *et al.*, 2012). A host of synthesis methods and parameters can be adopted to realise specific features of nanoparticles (Hajipour *et al.*, 2012). Among them the wet-chemical method is frequently used due to its simplicity and cost effectiveness (Topnani, Kushwaha and Athar, 2010).

Both copper oxide and zinc oxide have shown varying antibacteria activity against bacteria species (Zhang, 2011).They have been used in food packaging, wound healing and surface coatings due to their antimicrobial activities (Topnani, Kushwaha and Athar, 2010)(Konieczny and Rdzawski, 2012). However the antibacteria activities of these nanomaterials are yet to be compared against gram positive and gram negative bacteria species. In this study, investigation into the antibacteria activity on both gram negative and gram positive bacteria using copper oxide and zinc oxide nanoparticles are undertaken. The investigation will compare their respective antibacteria activity against *escherichia coli* (*e. coli*) and *staphylococcus aureus* (*s. aureus)* which are respective gram positive and gram-negative bacteria species. The copper and zinc oxides were synthesised by a common wet chemical method ensuring surfactant free nanoparticles to eliminate possible influences of surfactants on antibacteria activities.

1. **Experimental**

1.1`Synthesis of metal oxide nanoparticles

All chemicals were of analytical grade. Copper acetate (copper (II) acetate dihydrate) and zinc acetate (zinc acetate dihydrate) were used as precursors. Sodium hydroxide (grade) was used as the precipitating reagent. All chemicals were purchased from Sigma Aldrich, All aqueous solutions in the synthesis were prepared with deionised water from MilliQ (Milli-Q Water Systems, USA). The synthesis of nanometal oxide particles (metal oxide nanoparticles) was carried out by the facile wet chemical precipitation method. The wet chemical precipitation synthesis method convertes respective ionic solution into their insoluble nanometal oxide

precipitates with the aid of a precipitating reagent. Pure crystalline powdered nanometal oxides are obtained by separating precipitates from solution, drying and also calcination.

.. The following chemical equations describes the formation of nanometal oxides by the wet chemical synthesis:

$$(\boldsymbol{M(CH_2COO)aq} \rightleftharpoons \boldsymbol{M^+ + CH_2COO^-} \quad (1)$$

$$\boldsymbol{M^+ + NaOH \rightarrow MOH} \quad (2)$$

$$\boldsymbol{MOH \rightleftharpoons MO + H_20} \quad (3)$$

where in equation 1, ionic species M^+ is formed from the dissociation of $(\boldsymbol{M(CH_2COO)}$. NaOH in equation 2 is the precipitating reagent. MO which is a nanometal oxide is formed in 3. M is the metal component of the salt $(\boldsymbol{M(CH_2COO)}$.

1.1.1 Synthesis of copper oxide nanoparticles

0.1 M copper acetate was dissolved in 100ml of deionised water. The solution was continuously stirred at 700 rpm on a magnetic stirrer hot plate at 80 ^oC (H4000-HS, Benchmark Scientific, USA). The homogenous solution pH was adjusted to 11 with 2 M NaOH. The solution was continuously stirred at same speed and temperature for another sixty minutes. A black suspension with precipitates was formed, which is indicative of the formation of copper oxide (A. Kumar *et al.*, 2013). The temperature was allowed to gradually cool to room temperature at the same continuous stirring speed. The precipitates were separated by centrifugation and washed several times with distilled water to remove excess ions. The particles obtained were dried in an oven at 80 ^oC overnight. It was the then calcined at 500^oC to remove impurities which may be present on particles surfaces. The particles were subsequently characterised and applied for antibacteria activities. The formation of copper oxide nanoparticles is as described by the following chemical reactions 4-6:

$$(\boldsymbol{Cu(CH_2COO)_2)aq} \rightleftharpoons \boldsymbol{Cu^{2+} + CH_2COO^-} \quad (4)$$

$$\boldsymbol{Cu^{2+} + NaOH \rightleftharpoons Cu(OH)_2} \quad (5)$$

$$\boldsymbol{Cu(OH)_2 \rightleftharpoons CuO_2 + H_20} \quad (6)$$

1.1.2 Synthesis of zinc oxide nanoparticles

Similarly, 0.1 M zinc acetate was dissolved in 100 rpm of deionised water. A homogeneous solution was obtained after keeping the solution at 700 rpm on a hot magnetic stirrer plate (H4000-HS, Benchmark Scientific, USA) at 80 ^oC. The temperature and stirring speed were

kept constant throughout the synthesis period. A 2 M NaOH was added to the homogeneous solution to increase its pH to 11. A white precipitate was formed. The synthesis was allowed to continue for another sixty minutes. The precipitates were separated by centrifugation at 6000 rpm. The particles were severally washed to remove unreacted ions. They were dried at 80 ^{o}C for overnight and further calcined at 500 ^{o}C for 3 hours at a heating rate of 1 ^{o}C/S. The synthesised particles were successively analysed through a series of characterizations and utilized for antibiotic studies. The reactions that leads to the formation of zinc oxide nanoparticles is as described by equations 7-9;

$$(Zn(CH_2COO)_2)aq \rightleftharpoons Zn^{2+} + CH_2COO^{-} \quad (7)$$

$$Zn^{2+} + NaOH \rightleftharpoons Zn(OH)_2 \quad (8)$$

$$Zn(OH)_2 \rightleftharpoons ZnO + H_20 \quad (9)$$

1.2 Characterization of metal oxide nanoparticles

The properties of nanoparticles are affected by the synthetic method and parameters. In this study, the properties of the nanoparticles including the crystal structure, elemental composition, optical properties, morphology and the functional groups present were characterized using UV-Vis spectroscopy, X-ray diffraction and transmission electron microscopy analyses.

1.2.1 XRD analysis

The crystal structures for copper oxide and zinc oxide were respectively studied by an x-ray diffractometer (Empyrean, Malvern Panalytical, UK). The x-ray diffractometer carried out x-ray powder diffraction at a wavelength (λ) of 1.5418Å within a 2θ range of 10^{o} to 80^{o}.

1.2.2 UV-Vis spectroscopy analysis

In this study the UV-Vis Spectrophotometer (Genesys 150 UV-Vis, ThermoFisher Scientific, USA) was adopted to obtain the UV-Vis spectrum of nanometal oxides. The measurement was done at a scanning range of 200 nm to 800 nm. A quartz cuvette filled with 1 ml aqueous suspension of respective nanometal oxide was analysed whiles using deionised water from Milli-Q as the blank solution for the measurement. The UV-Vis spectrum of nanoparticle is

highly dependent on the particle size and shape which are determined by the fabrication method and the optimized parameters in the technique.

1.2.3 Transmission electron microscope (TEM) analysis of nanoparticles

TEM (JEOL 2010, JEOL Ltd., USA) was used to observe the morphologies of the synthesized nanoparticles. A minute sample of the synthesized particles were re-dispersed in an appropriate amount of water. The aqueous suspension was sonicated to overcome agglomeration resulting from drying the particles. A few drops of one to two of the sonicated suspension was immobilized on a carbon grid. The immobilized particles were evaporated and observed with TEM after it had dried.

1.2.4 FTIR analysis of metal oxide nanoparticles

A minute quantity of fine CuO and ZnO powders were separately placed on the clean infrared transparent surface of the FTIR instrument. The infrared scan was performed within the range of 4000~400 cm^{-1}.

1.3. Antibacteria testing

The antibacteria applications of nanometal oxides were carried out under sterile conditions inside a laminar flow cabinet. All media cultures, pipette tips water and glassware used for the microbiology testing were sterilized by autoclaving (UMB220 Benchtop Autoclave, Astell, USA) at 121 ^{o}C for 15 minutes. *Escherichia Coli* (*e. coli*) which is a gram negative bacteria and the *staphylococcus aureus* (*s. aureus*), a gram positive bacteria were used for the antibacterial studies.

1.3.1 Disk diffusion assay

Disk diffusion assays were prepared by the Kirby Bauer method. In this method, aqueous stock solutions of CuO and ZnO were appropriately prepared. Serial dilutions were prepared from the stock solution to obtain varying concentrated solutions of the nanometal oxides. Filter papers of approximately 6 mm were inserted into each aqueous suspension of nanoparticles and allowed to completely soak briefly. Subsequently, Mueller Hinton agar (MHA) media culture was prepared by dissolving 38 g of MHA in one litter of deionised water. The solution

was autoclaved for 15 minutes at 121^{o}C. Disk plates of about 9 cm diameter were filled with a quantity of the prepared MHA in a sterilized laminar flow chamber and allowed to solidify shortly. *E. coli* and *s. aureus* were plated onto the agar plates by streaking. The paper disks were placed on the agar plate using a sterilize forceps. The plates were incubated at 37 ^{o}C overnight. Zones of inhibition surrounding the filter disc as a result of antibacteria activity of the nanoparticles were observed and measured with a millimetre rule and the measurements recorded accordingly.

1.3.2. Bacteria growth kinetic assay

The bacteria growth kinetic assay was carried out to observe the periodic growth of bacteria in a liquid broth. In this approach, optical density (OD) of the prepared assay were measured at regular interval and the changed in optical density which corresponds to bacteria growth were recorded. The assay was prepared by pipetting 60 ul of broth into a 96 well plate. To this, 20ul (20 ul) of bacteria (*E. coli or S. Aureus*) at a concentration of 0.5 MacFarlad standard were individually added. Various concentrations of nanoparticles (1 mg/ml, 0.5 mg/ml, 0.25 mg/ml, 0.1 mg/ml, and 0.05 mg/ml) of 20 ul were added and the inoculum incubated at 37 ^{o}C on an orbital shaker at 225 rpm. Optical density of inoculum was recorded by measuring with the UV-Vis spectroscopy (VarioSCAN microplate reader) at period intervals of two hours.

The following contents were made for each bacteria: Broth media, broth media + Bacteria; and finally Broth media +Bactria+ Nanometal oxides. Each bacteria species was subjected to different concentrations (1 mg/ml, 0.5 mg/ml, 0.25 mg/ml, 0.1 mg/ml, and 0.05 mg/ml) of nanometal oxides.

2. Results and discussions

2.1 X-ray Diffraction (XRD) analysis

The XRD patterns reveal that the as-synthesised nanometal oxides were fine and free of impurities (Figure 1). There was no spectra peak relating to impurities that was found in any pattern. The diffraction patterns demonstrate sharp peaks as indication of the good crystallinity of the nano powders. The XRD patterns obtained for copper oxide are in exact agreement with the monoclinic phase of copper oxide. The spectra peaks had precise correlation with that of the monoclinic phase. Figure 1 shows the XRD spectra pattern for copper oxide (Dahrul, Alatas and Irzaman, 2016).

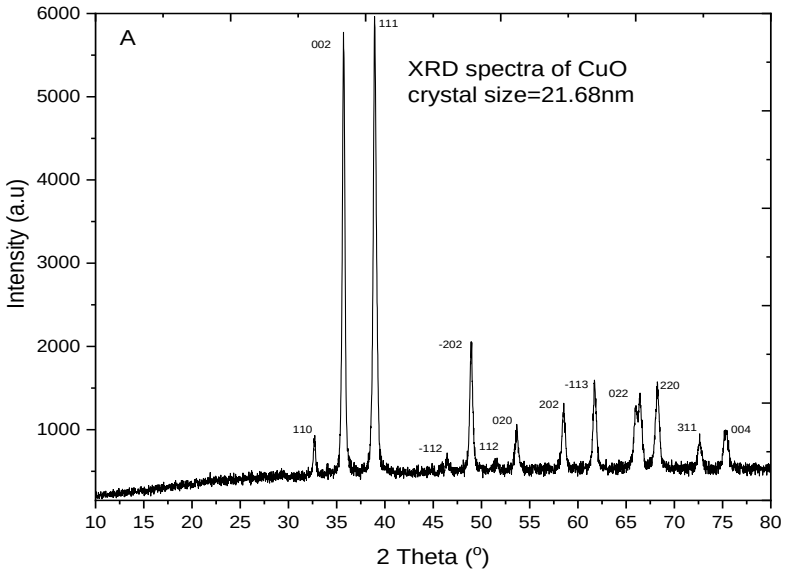

Figure 1: XRD spectra pattern for copper oxide.

Figure 2 illustrates the patterns for zinc oxide. The diffraction peaks of zinc oxide correctly matched the hexagonal wurtzite structure of zinc oxide. Scherer's equation was used to estimate the crystal sizes for copper oxide and zinc oxide as 21.68 nm and 21 nm respectively. The possible explanation to the difference between the crystal size recorded by XRD and the particle size recorded by TEM analysis is agglomeration.

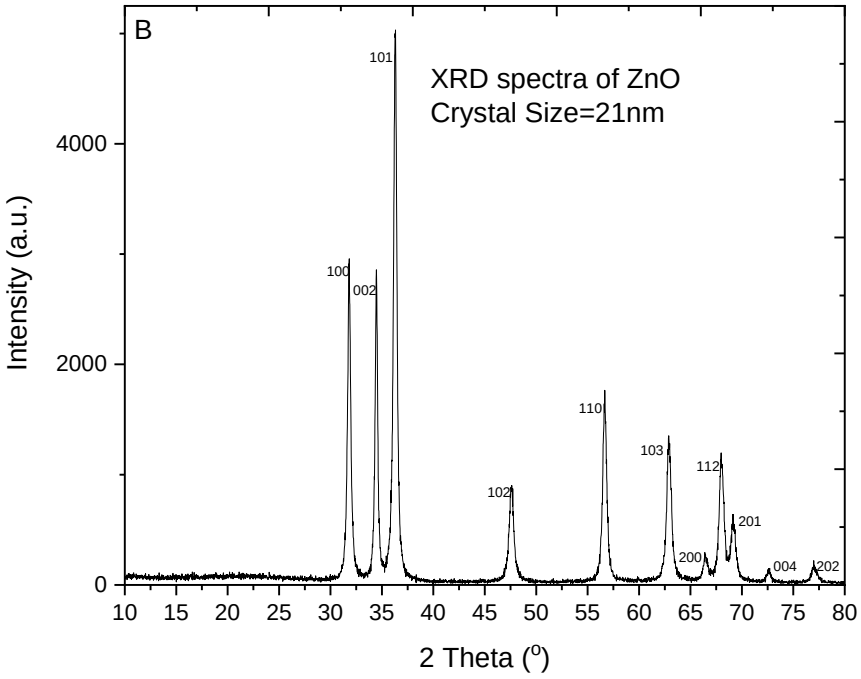

Figure 2: XRD spectra pattern for Zinc Oxide.

2.2 UV-Vis spectroscopy analysis of nanometal Oxides

The UV-Vis spectrum of nanometal oxides showed peaks within the range of 200 nm to approximately 400 nm (Caro, 2017). A UV-Vis analysis of the synthesised copper oxide and zinc oxide nanoparticles is shown in Figure. 1. The UV-Vis spectrum of absorbance (Abs.) versus wavelength showed peak absorbance at 275 nm which is an indication of electron transition from a valence band to a conduction band. This observation is attributed to the transition from the 2_p of oxygen to the 4_s of Cu^{2+} (Dahrul, Alatas and Irzaman, 2016). The broad range of the spectrum which ranges from the ultraviolet (UV) to visible light is typical of nanometal oxides. However, their highest peak occurred in the UV region (Mondal, 2017). The broad range also signifies that nanoparticles have a range of sizes and shape (Khashan, Jabir and Abdulameer, 2018).

Copper oxide is a direct-band gap materials (Mugwanga *et al.*, 2013). When a semiconductor such as nanometal oxide absorbs energy photon greater than its band gap energy, it causes the transfer of electrons from the valence band to the conduction band (Wang *et al.*, 2016). If the electron momentum in the transition process is conserved, then the material has a direct band gap (Das and Alford, 2013). The absorbance of the material corresponds to the wavelength and the energy band gap (Kumar and Rani, 2013). The absorption coefficient and the energy of direct-band gap materials are related by the Tauc's equation (Das and Alford, 2013). Hence the optical band gap of the spectrum is obtained by a plot of $(\boldsymbol{ahv})^{\boldsymbol{2}}$ against $\boldsymbol{hv}(\boldsymbol{eV})$**.** Where 'a' is the absorption coefficient and 'h' and 'v' are respectively the plank's constant and the frequency of the waveform. The bandgap with respect to antibacteria activity provides information on the energy efficiency to the production of electrons leading to ionic species release which are considered toxic to cells (Xiu *et al.*, 2012). The Tauc's relation in equation 10 describes a relationship between $(\boldsymbol{ahv})^{\boldsymbol{2}}$and the band gap energy $\boldsymbol{hv}(\boldsymbol{eV})$ in direct band gaps.

$$(\boldsymbol{ahv})^{\frac{\boldsymbol{1}}{\boldsymbol{n}}} \propto \boldsymbol{hv} - \boldsymbol{E_g} \qquad (10)$$

where n is the order of refractive index. Thus, the x intercept of the waveform is the band gap energy.

The energy band gap of copper oxide nanoparticles was calculated to be 2.7 nm as indicated in figure 3. The band gap obtained is in agreement with previous works (Wang *et al.*, 2016).

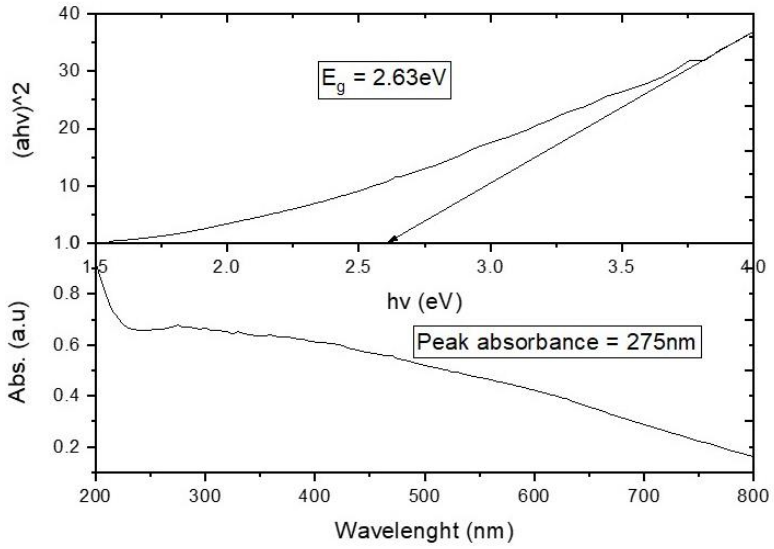

Figure 3: UV-Vis spectrophotometer of Copper Oxide showing peak absorbance and its bandgap energy.

Zinc oxide nanoparticles shows a sharp peak at 355 nm (Figure 4). This is due to the electron transfer across its band-gap. Electron transition occurs between the valence band and its conduction band. The 2d band of oxygen is the valence band of ZnO whiles the 3_d orbital of Zn^{2+} is the conduction band (S. S. Kumar *et al.*, 2013). Implementing the same Tauc's equation for finding the band-gap energy. 3.22 eV was realised as the energy-band gap for the zinc oxide. A similar energy band-gap for has been reported for zinc oxide as a direct band gap with a wide band gap (Varughese, Jithin and Usha, 2015).

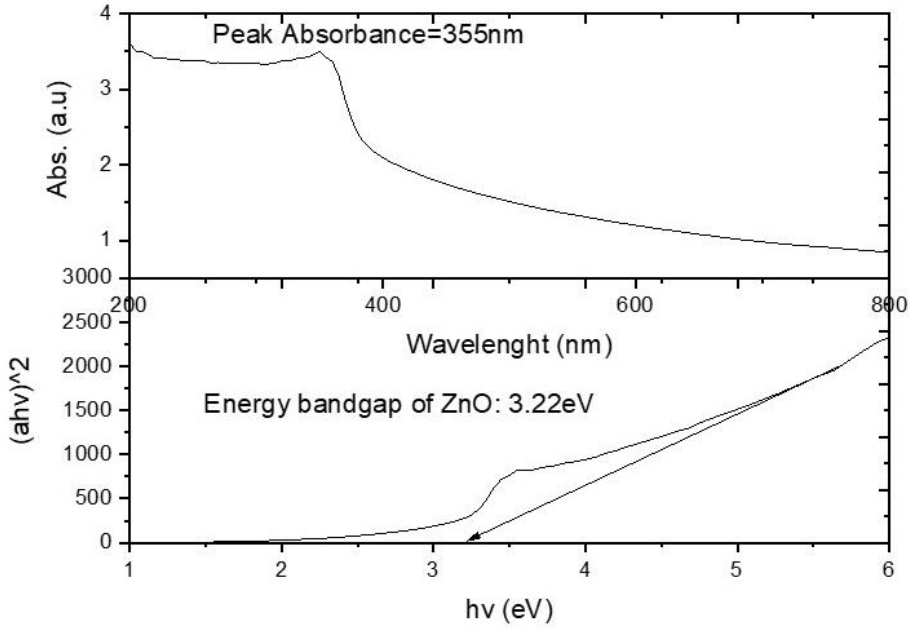

Figure 4: UV-Vis spectrophotometer of Zinc Oxide showing peak absorbance and its bandgap energy.

The semiconductor materials have the ability to promote electrons from the valence band to the conduction band with the help of photons from a light source. This creates electron-hole pairs. The electrons in the conduction band and the holes in the valence band interact with bacterial species to generate reactive oxygen species (ROS). ROS is responsible for the destruction of cell membranes and organelles. Thus, the antibacterial activity of nanoparticles is enabled by the generation of ROS activities.

A lower band gap means the metal oxide (nanoparticles) can obtain the necessary photon at lower energy wavelength to cause ROS activities. A higher band gap means the energy can be obtained in a higher energy. A lower energy can be the visible light which can be obtained from normal daylight and a higher energy may be ultraviolet light (UV) which can be obtained by extended aid. The UV-Vis spectrum of copper oxide and zinc oxide shows that copper oxide has lower energy band gap relative to zinc oxide. This means that copper oxide in the presence of visible light can more easily produce electrons in solution than zinc oxide. Thus copper oxide in such a condition is expected to result in more ROS activity hence higher antibacteria activity as compared to zinc oxide.

2.3 Transmission electron microscope (TEM) analysis of nanoparticles

The TEM micrographs reveal that the wet-chemical aqueous precipitation synthesis method produced copper oxide nanorods. As demonstrated in Figure 5, the synthesized nanoparticles agglomerated in bundles or clusters of nanorods. The nanorods occurred in lengths varying from 70 nm to 170 nm. The average length of the nanorods was observed to be 100 nm. The width of the nanorods was found to range from 8nm to 36 nm with 14 nm as the average width of the nanorods.

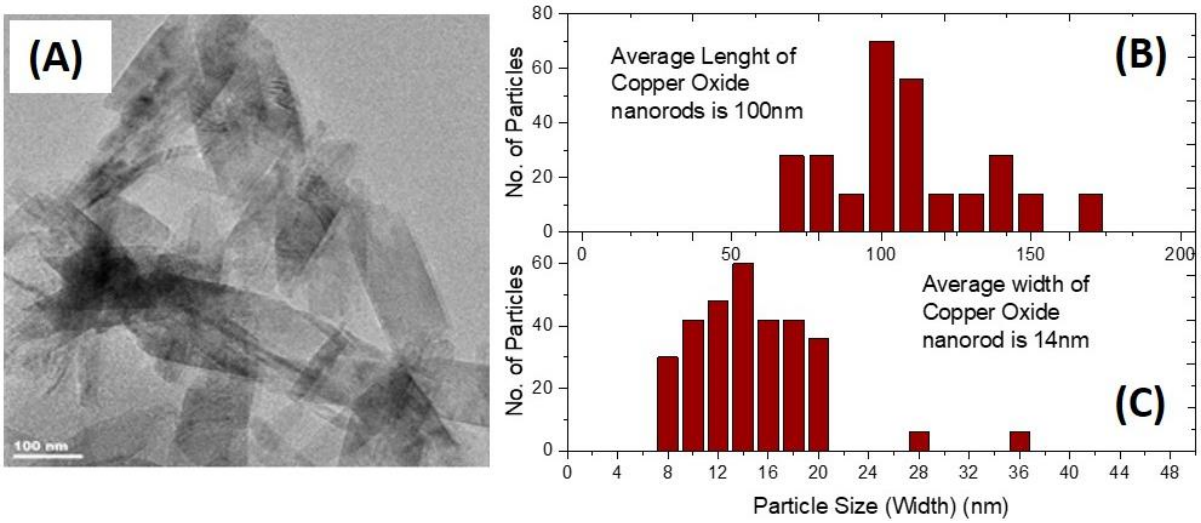

Figure 5: (A) A TEM micrograph of copper oxide nanoparticles. (B) A histogram distribution of the length of the nanoparticles (C) A histogram showing the distribution in the width of the nanoparticles.

The TEM micrograph of zinc oxide nanoparticles is shown in figure 6. Unlike copper oxide, wet-chemical aqueous precipitation synthesis of zinc oxide did assume a more spherical shape. The particles were also however more broadly distributed in size. The size analysed by Image J showed that it ranged from 10nm to 35nm. The average size was 15 nm. Wet chemical aqueous precipitation synthesis of nanometal oxides has revealed that whiles it produces nanorod copper oxides, it however creates zinc oxides that are predominantly spherically shapes. The zinc oxide produced are more widely distributed in size as compared to the copper oxide nanorods.

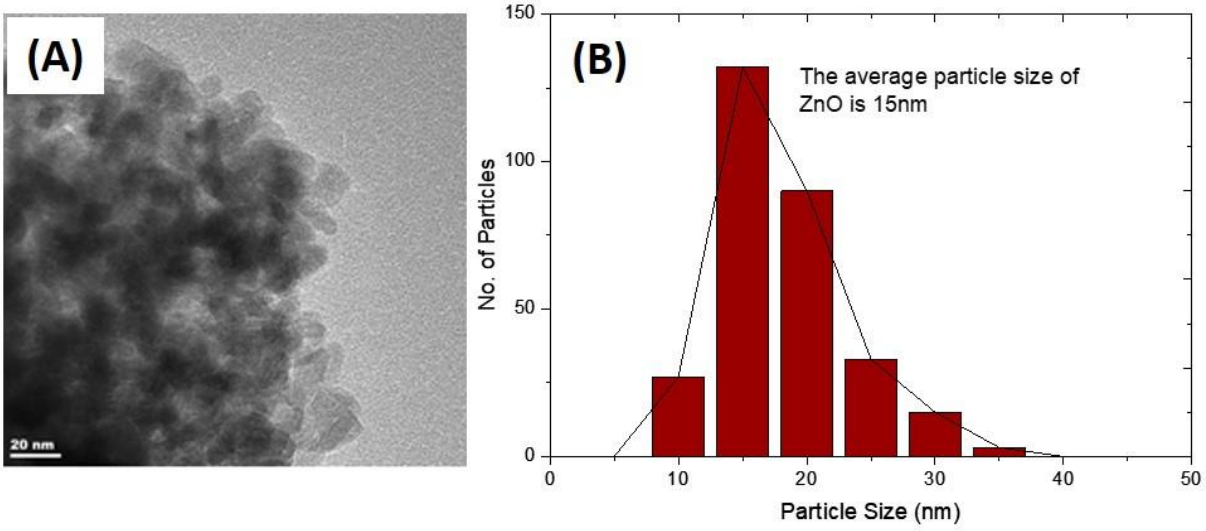

Figure 6: (A) A TEM micrograph of zinc oxide nanoparticles. (B) A histogram distribution of the size of the zinc oxide nanoparticles.

2.4 FTIR analysis of metal oxide nanoparticles

The infrared spectra of copper oxide nanorods is shown in Figure 5a. The peak observed at 596 cm^{-1} is a band associated with the stretching vibration of Cu-O bonds. The absorption bands within 1350 cm^{-1} and 1650 cm^{-1} are indications of atmospheric CO_2. Spectra bands occurring between 2800 and 3500 cm^{-1} corresponds to O-H bonds. O-H bonds with very low bands are due to the minute presence of a moisture content. The FTIR in Figure 7 confirms that copper oxide was synthesised and confirmed by the presence of Cu-O bond. The FTIR spectra analysis of zinc oxide is shown in figure 5b. The absorption band at 863 cm^{-1} is an indication of Zn-O vibration.

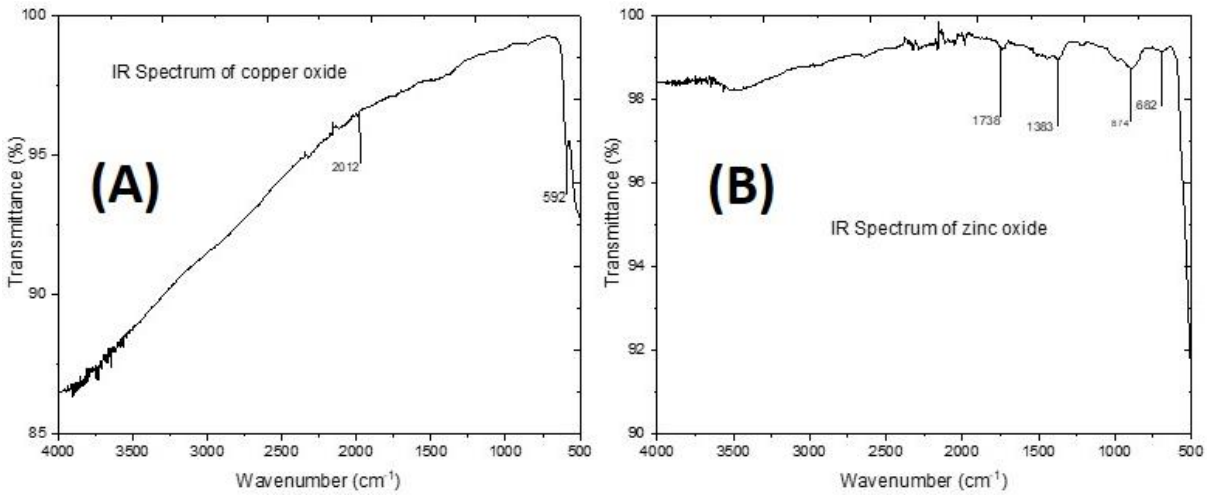

Figure 7: Infrared spectra analysis of (A) Copper oxide and (B) Zinc oxide nanoparticles.

The FTIR spectra shows that there were no surfactant present on the surface of both nanoparticle samples. This can be deduced from the absence of significant amount of any organic species on the surface of nanoparticles. Hence surfactant free nanoparticles were synthesised which is important to study the original contribution of either nanoparticles in antibacteria activity.

2.5 Antibacteria study of nanometal oxides against bacteria species

2.5.1 Disk diffusion studies

The Kirby Bauer Disk diffusion method was employed to investigate antibacteria activity of nanometal oxides on bacteria species. Aqueous suspension of nanometal oxides ranging from 5 mg/ml to 0.01 mg/ml were tested on *e. coli* and *s. aureus* which represent gram positive and gram negative bacteria species. Nanometal oxides demonstrated varying activity against the gram negative and gram positive bacteria species.

Figure 8 indicates that copper oxide showed varying activity on *e. coli* which is a gram negative bacteria.

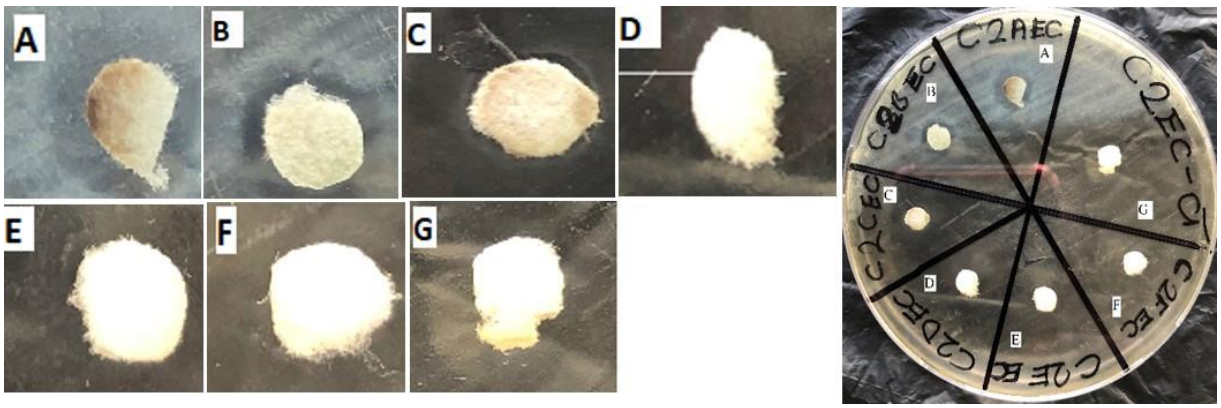

Figure 8: Antibacteria activity of copper oxide on *e. coli.*

The activity depended on the concentration of copper oxide. Copper oxide concentrations of 5 mg/ml and 2 mg/ml showed significant activity on *e. coli*. Copper oxide concentrations of 1 mg/ml had a marginal activity on E. coli whiles concentrations lower than 1 mg/ml had no significant activity on the *e. coli*. Copper oxide however showed higher activity on *s. aureus*. Copper oxide concentrations from 5 mg/ml to 0.25 g/ml showed activity on *s. aureus* as demonstrated in Figure 9.

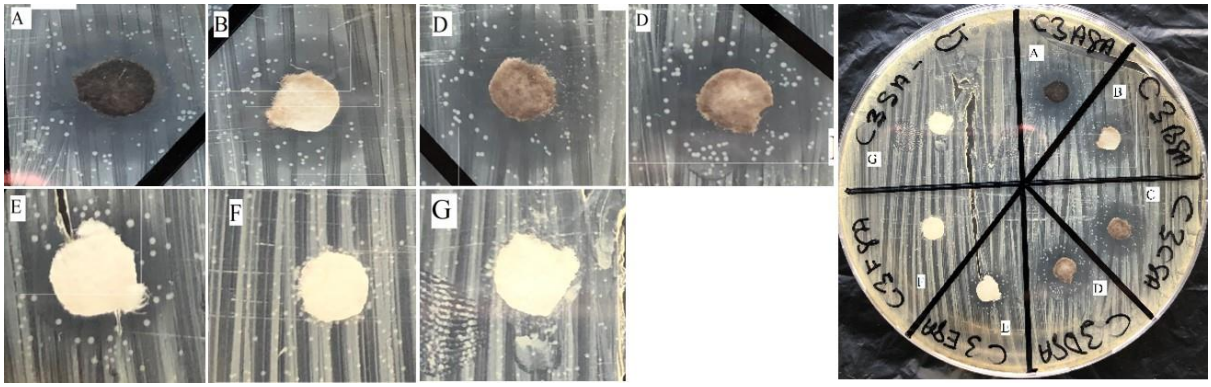

Figure 9: Antibacteria activity of copper oxide on S. Aureus.

Figure 10 shows a histogram comparing the activity of copper oxide on *e. coli* and *s. aureus*.

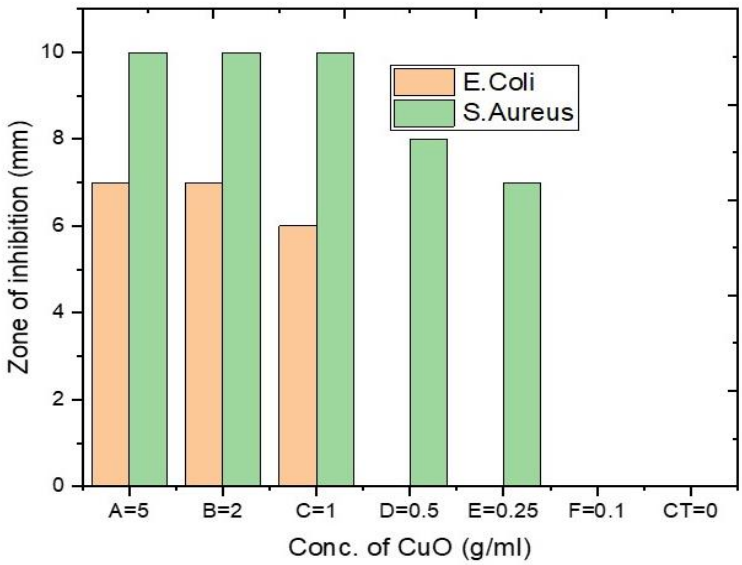

Figure 10: A comparative assessment of the activity of copper oxide on *e. coli* and *s. aureus*.

E. coli was more resistive to the antibacteria activity of copper oxide as compare to *s. aureus* Zinc oxide nanoparticles was similarly tested on *e. coli* and *s. aureus*. Figure 11 reveals the activity of zinc oxide nanoparticles on *e. coli*. The results demonstrates that zinc oxide had no effect on *e. coli*. All the concentrations of zinc oxide from 5 mg/ml to 0.01 mg/ml showed no activity against *e. coli*. Thus, all the various concentrations of zinc oxide nanoparticles recorded no zone of inhibition when tested on *e. coli*.

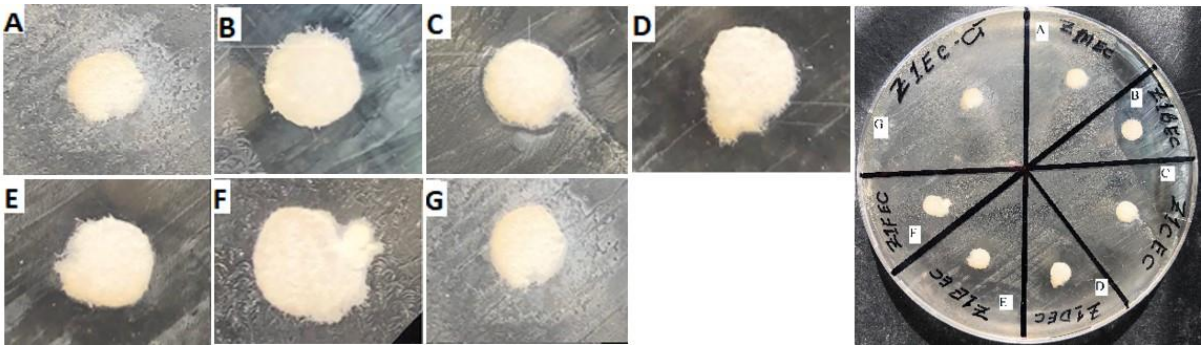

Figure 11: Antibacteria activity of zinc oxide on *e. coli*.

Zinc oxide nanoparticles were likewise tested on S. Aureus. Unlike its performance on *e. coli*, zinc oxide nanoparticles showed effect on *s. aureus*. The various concentrations of nanoparticles ranging from 5 mg/ml to 0.01 mg/ml showed an effect on *s. aureus*. The effect shown on *s. aureus* increased with increasing concentration. Figure 12 shows the activity of zinc oxide on *s. aureus*.

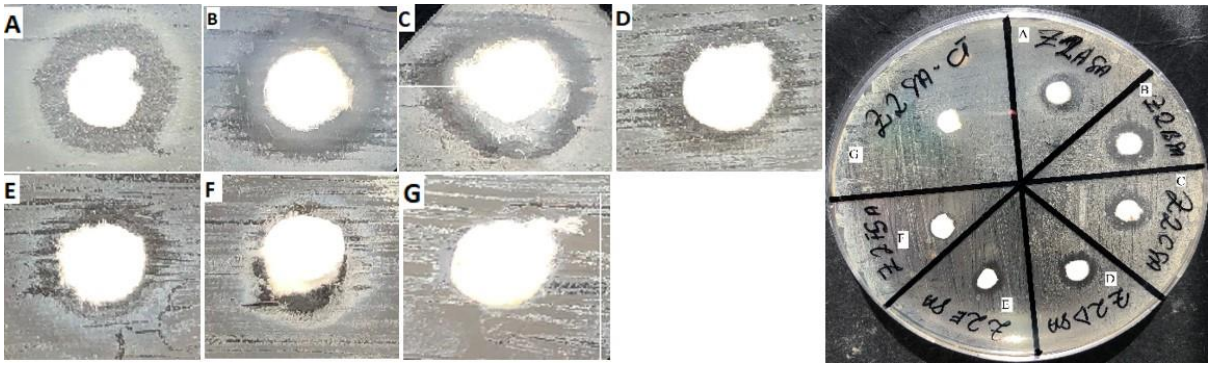

Figure 12: Antibacteria activity of zinc oxide nanoparticles on *s. aureus*.

Whiles zinc oxide showed activity against S, Aureus it was ineffective against *e. coli*. Figure 13 is a histogram of the activity of zinc oxide on *e. coli* and *s. aureus*.

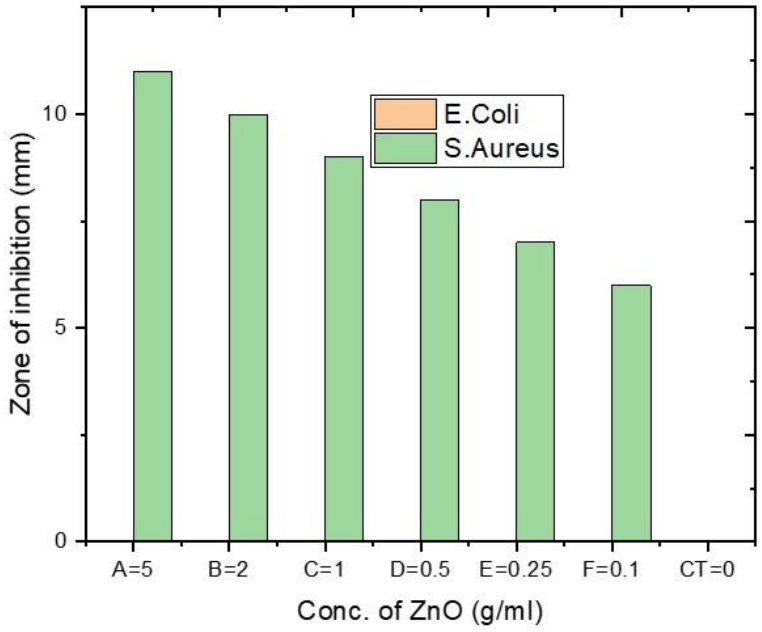

Figure 13: Histogram showing the relative activity of zinc oxide on *e. coli* and *s. aureus*.

The Kirby Bauer disk diffusion method of antibacteria testing revealed that *e. coli* strain ATCC25923 is resistive to nanometal oxides of zinc oxide. Copper oxide nanoparticles were slightly effective against the nanoparticles. Meanwhile *s. aureus* strain ATCC25923 tested with the same sets of nanoparticles indicated that the nanoparticles were efficient in resulting in cell death in the order of increasing concentration. Figure 14 compares the efficiency of zinc oxide and copper oxide nanoparticles against *e. coli* and *s. aureus*.

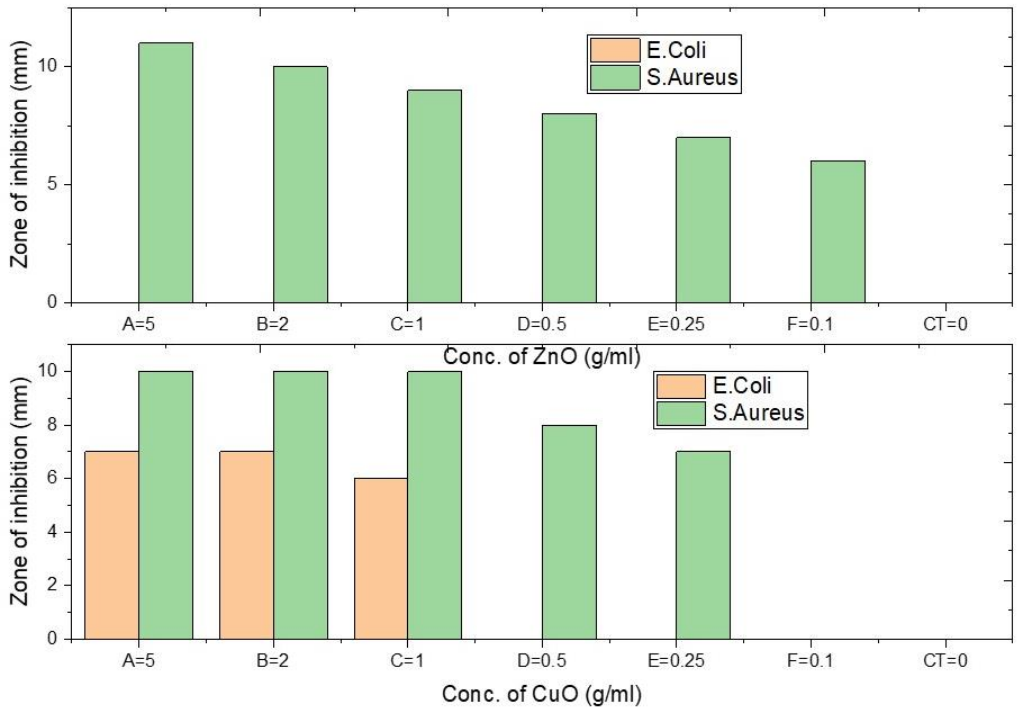

Figure 14: A histogram showing the comparison of the antibacteria activity of copper oxide and zinc oxide on *e. coli* and *s. aureus*.

2.5.2 Bacteria growth kinetic study

To understand the kinetics of anti-bacterial activity, liquid broth assay provides a more idle method. Liquid broth assay which is also popularly called the broth microdilution examines changes in the growth of bacteria in a broth (liquid) assay by measuring its optical density. The optical density of the assay provides an estimation of the amount of bacteria cells present in the assay. Spectrophotometer measure optical density of bacteria cells by recording the concentration of the cells at an absorbance of 600 nm. Meanwhile, nanometal oxides may have absorbance within the range of 600 nm which is excluded from the analysis. The antibacteria kinetics studies provides information on the rate of activity of metal oxides on bacteria species.

The growth kinetics studies began with the same number of bacteria cells for both gram positive and gram-negative bacteria. $6*10^6$CFU was used as the starting amount of bacteria. Corresponding changes in the initial bacteria density was measured by noting its corresponding changes in optical density at 600 nm. The bacteria growth dynamics studies was with and without the presence of nanometal oxides. Assays without nanometal oxides was used as a reference for antibacteria studies. Thus the dynamic bacteria growth depended on the

antibacteria metal oxides. Varying concentrations (1 mg/ml, 0.5 mg/ml, 0.25 mg/ml, 0.1 mg/ml, 0.05 mg/ml) of both copper oxide and zinc oxide were applied on both the gram positive and gram negative bacteria. The bacteria growth kinetic study is shown in figure 15.

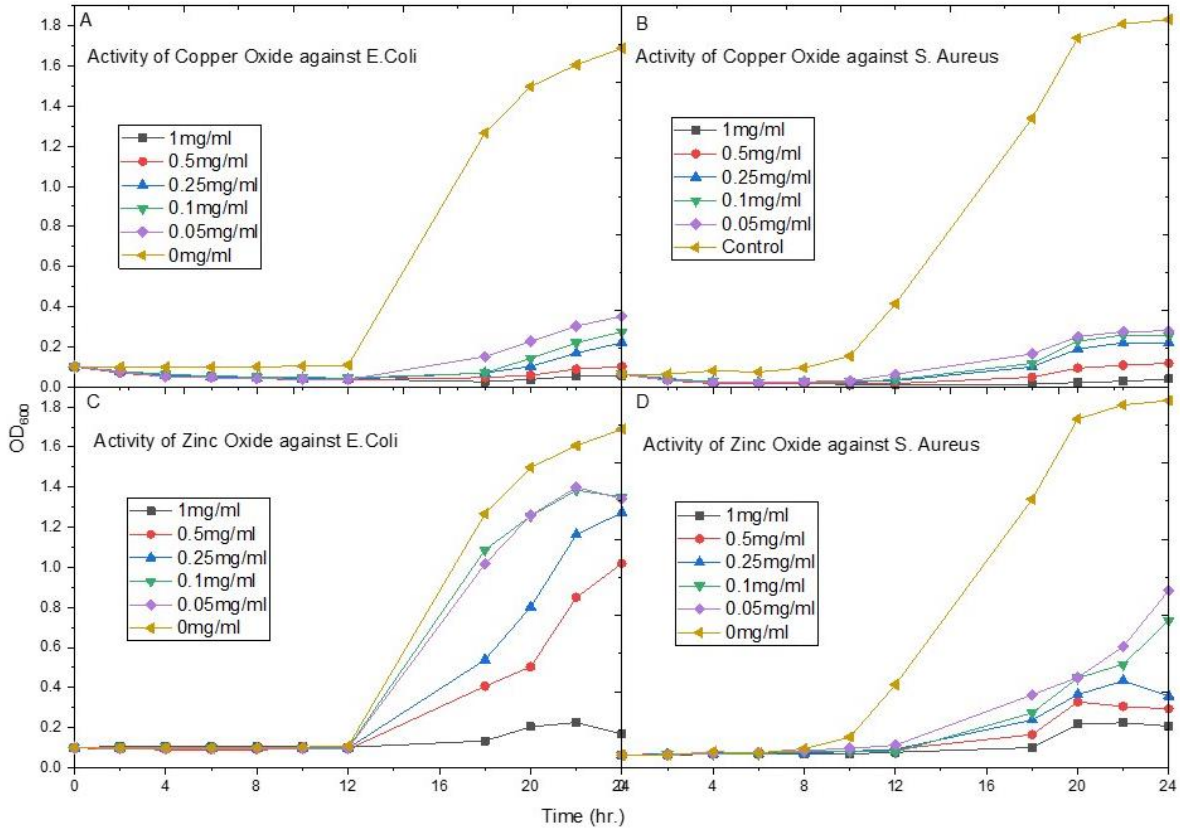

Figure 15: Dynamic growth kinetic study of the activity of: (A) Copper Oxide against *e. coli* (B) Copper Oxide against *s. aureus* (C) Zinc Oxide AGAINST E. coli and (D) Zinc Oxide against S. aureus.

Copper oxide showed relatively higher activity against both *e. coli* and *s. aureus*. The activity of both copper oxide and zinc oxide was more effective against S. aureus than E. coli. A similar results have been reported by other authors on the relative efficiency of nanoparticles against gram positive bacteria such as *s. aureus* than gram negative bacteria such as *e. coli* (Jung *et al.*, 2008). Although gram positive bacteria have comparatively thicker cell wall which is expected to make them more resistive to nanoparticles, recent works hypothesised that the gram negative bacteria of *e. coli* possess flagellum which could cause the agglomeration of nanoparticles (Salas Orozco *et al.*, 2019). The agglomeration of nanoparticles significantly reduces their toxic effect (Roselina and Azizan, 2012). The results obtained in the optical density test agrees with

the results of the disk diffusion test. In the disk diffusion test, copper oxide nanoparticles again showed enhanced activity in both bacteria species than zinc oxide.

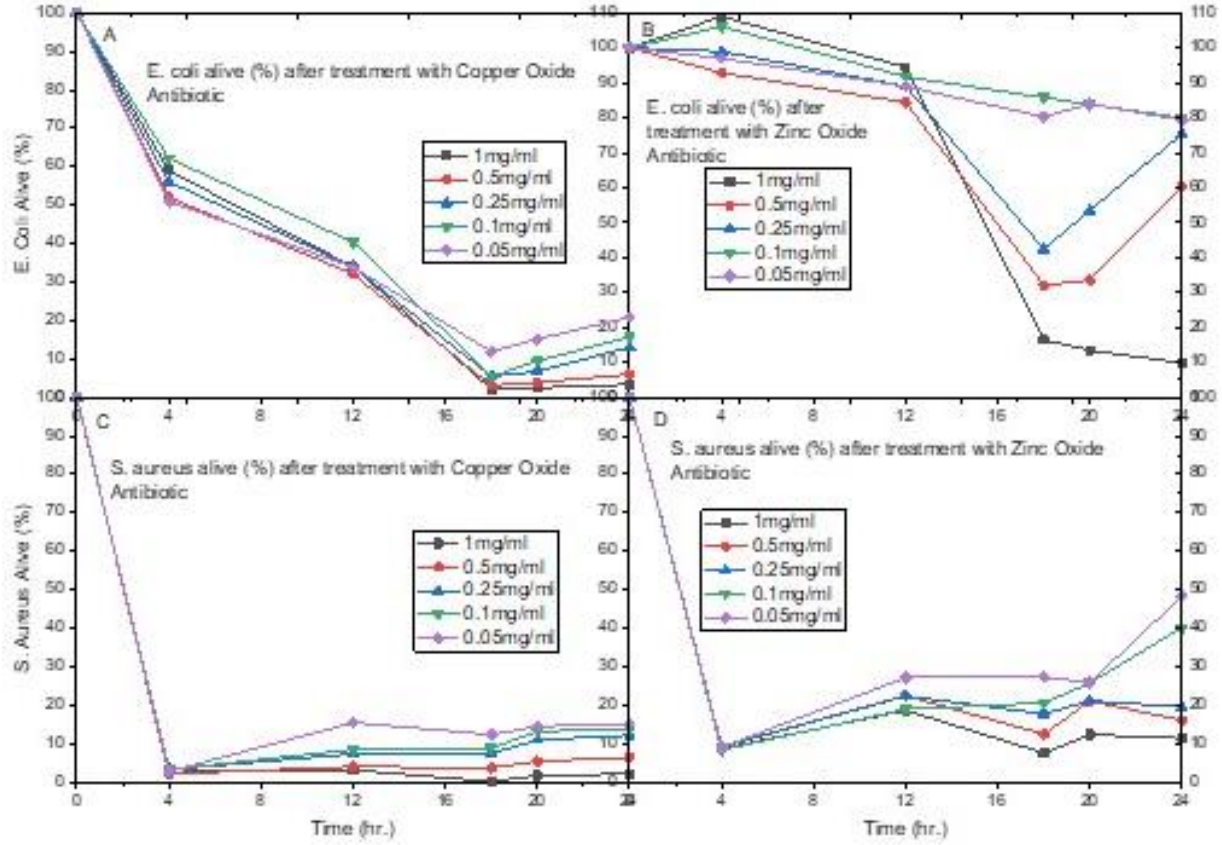

Figure 15: Dynamic growth kinetic study on (A) *e. coli* alive (%) after treatment with copper oxide (B) *e. coli* alive (%) after treatment with zinc oxide (C) S. aureus alive (%) after treatment with copper oxide (D) *s. aureus* alive (%) after treatment with zinc oxide.

Figure 16 demonstrates the amount of bacteria cells present in the inoculum with respect to time after treatment with the respective nanoparticles at their varying concentrations. It can be realised from the figure that in the case of *e. coli*, the dynamic kinetic growth curve has a gradual slope. It reaches its minimum point after a prolong time of treatment. This means that the antibiotic effect of the nanoparticles takes a considerable length of time to result in the death of *e. coli* cells. Thus, *e. coli* cells are tolerable to the antibiotic effect of the nanoparticles for a considerable length of time. It can also be deduced from the *e. coli* (%) versus Time (hr) plot that copper oxide had the most effect on *e. coli* as compared to Zinc oxide. More *e. coli* cells remained alive in the respective inoculum treated with nanoparticle concentrations of zinc

oxide as compared to those of copper oxide. The *e coli* cells were thus more resistive to zinc oxide nanoparticles than copper oxide nanoparticles.

In the case of *s. aureus*, the *s. aureus* alive (%) versus Time (hr) plot has a very sharp slope. That is *s. aureus* cells were very susceptible to both nanoparticles. Similarly, it is also observed that copper oxide nanoparticles were comparably more toxic to the *s. aureus* cells hence relatively less amount of *s. aureus* cells remained alive with respect to time.

A similar observation was made in the disk diffusion test. Copper oxide nanoparticles were comparably more effective on both *e. coli* and *s. aureus* as compared to zinc oxide.

Figure 16 shows the efficiencies of the respective nanoparticles on the different bacteria species. The efficiencies of the nanoparticles were each observed to be dependent on the concentration of the nanoparticle used for bacteria treatment. The efficiency in the case of each nanoparticle increased with increasing the nanoparticle concentration. A similar observation is common among experimental studies in drug-pathogen relationships. In the case of the disk diffusion, a similar pattern of antibiotic activity was observed. The effect of the disk carrying antibiotic nanoparticles was dependent on the concentration of nanoparticle suspension in which it was immersed or dipped. The higher the concentration the higher the amount of nanoparticle or nanoparticle ions immobilised on the disk for antibacteria activity.

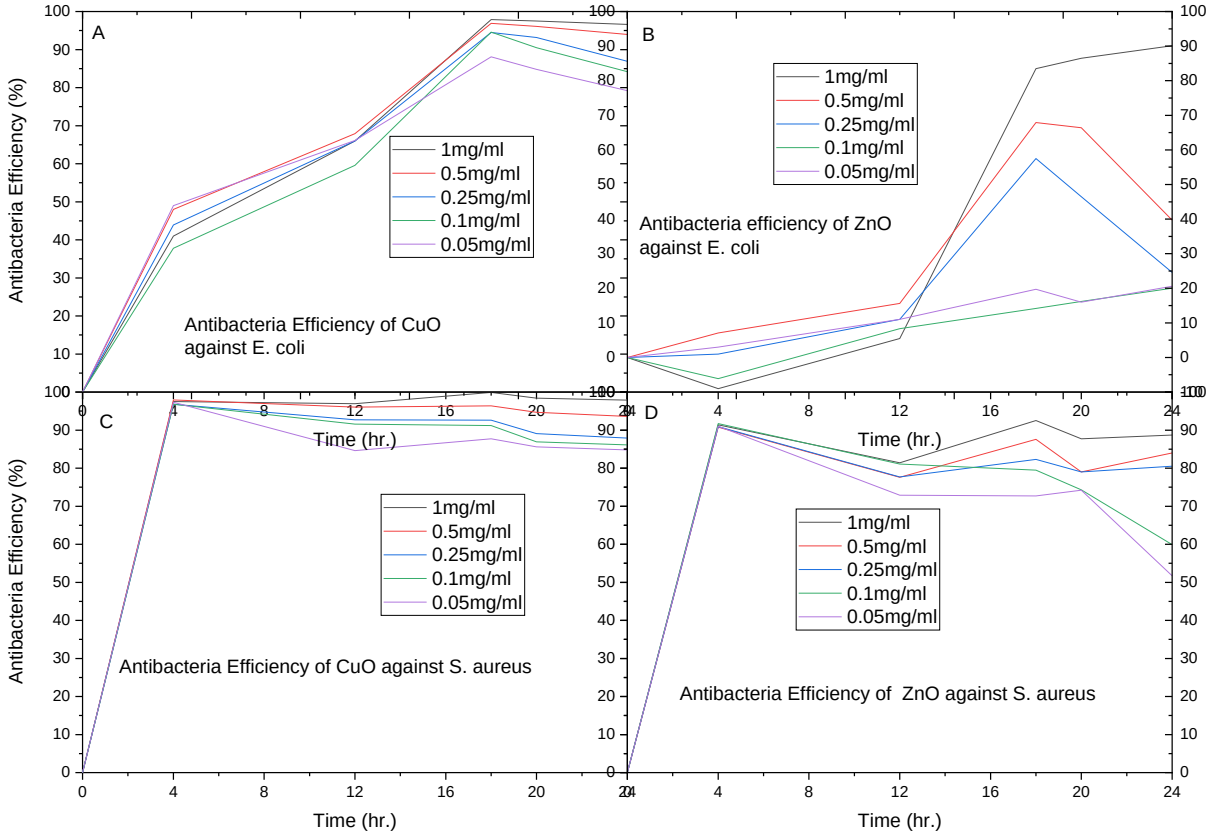

Figure 16: Dynamic growth kinetic study on (A) Antibacteria efficiency of copper oxide against *e. coli* (B) Antibacteria efficiency of zinc oxide against *e. coli* (C) Antibacteria efficiency of copper oxide against *s. aureus* (D) Antibacteria efficiency of zinc oxide against *s. aureus.*

According to figure 16, copper oxide nanoparticles at the concentration of 1 mg/ml could achieve antibacteria efficiency of approximately 99 % against both *e. coli* and *s. aureus.* Zinc oxide achieved 90 % and 89 % respectively for *e. coli* and *s. aureus* at the same concentration. Hence, coper oxide demonstrated higher antibacteria activity against both *e. coli* and *s. aureus* as compared to zinc oxide.

3. Conclusion and future work

In this study, facile method was used to achieve the complete synthesis of ultra-fine nanometal oxide particles. The synthesis method which was fast, inexpensive and easy to carry out was also easy to separate from suspension for preparation for characterization studies. The characterization results showed that the easily synthesised nanometal oxides were void of impurities and achieved high degree of crystalline nature with diffraction peaks well indexed

to known and hypothesised patterns. The facile synthesised particles achieved optical properties conforming to their existing kinds with particles size below 100 nm which categorises them as nanoparticles. The synthesised particles were further characterised to free of surfactant hence their antibacteria activity would be unaided by organic species which could also possess antibacteria activity. The antibacteria activity of the nanometal oxides on gram negative bacteria and gram positive which were respectively E. coli and S. aureus showed that both nanometal oxides of copper oxide and zinc oxide could inhibit bacteria activity dependent on their concentration. The antibacteria activity increased directly proportional to their concentration. However, this study revelation demonstrates two different but complementing methods of antibacteria testing which are the disk diffusion and the optical density test that copper oxide possessed a comparatively higher antibacteria on both gram negative bacteria which is *e. coli* and gram positive bacteria which is *s. aureus*. The results is useful for the synthesis, characterization and the relative antibacteria efficiencies of two of the most popular metal oxide antibacteria agents. Further studies may be carried into the impart of different synthesis methods on the properties and the effects of these two widely considered metal oxide nanometal oxides.

References

Agnihotri, S., Mukherji, Soumyo and Mukherji, Suparna (2014) 'Size-controlled silver nanoparticles synthesized over the range 5–100 nm using the same protocol and their antibacterial efficacy', *RSC Adv.*, 4(8), pp. 3974–3983. doi: 10.1039/C3RA44507K.

Ahmed, S. *et al.* (2016) 'REVIEW A review on plants extract mediated synthesis of silver nanoparticles for antimicrobial applications : A green expertise', *Journal of Advanced Research*. Cairo University, 7(1), pp. 17–28. doi: 10.1016/j.jare.2015.02.007.

Caro, C. A. De (2017) 'UV / VIS Spectrophotometry', *Mettler Toledo*, (November), pp. 4–14.

CDC, C. for D. C. (2018) 'Diarrhea: Common Illness, Global Killer', *Fact Sheet*, pp. 1–4. Available at: https://www.cdc.gov/healthywater/pdf/global/programs/globaldiarrhea508c.pdf%0Ahttps://www.cdc.gov/healthywater/global/diarrhea-burden.html.

Chandraker, K. *et al.* (2015) 'Radical Scavenging Efficacy of Thiol Capped Silver Nanoparticles', *Journal of Chemical Sciences*, 127(12), pp. 2183–2191. doi: 10.1007/s12039-

015-0968-x.

Dahrul, M., Alatas, H. and Irzaman (2016) ‘Preparation and Optical Properties Study of CuO thin Film as Applied Solar Cell on LAPAN-IPB Satellite’, *Procedia Environmental Sciences*. Elsevier B.V., 33, pp. 661–667. doi: 10.1016/j.proenv.2016.03.121.

Das, S. and Alford, T. L. (2013) ‘Structural and optical properties of Ag-doped copper oxide thin films on polyethylene napthalate substrate prepared by low temperature microwave annealing’, *Journal of Applied Physics*, 113(24). doi: 10.1063/1.4812584.

El-Trass, A. *et al.* (2012) ‘CuO nanoparticles: Synthesis, characterization, optical properties and interaction with amino acids’, *Applied Surface Science*. Elsevier B.V., 258(7), pp. 2997–3001. doi: 10.1016/j.apsusc.2011.11.025.

Feng, Q. L. *et al.* (2000) ‘A mechanistic study of the antibacterial effect of silver ions on Escherichia coli and Staphylococcus aureus’.

Foldbjerg, R. *et al.* (2015) ‘Toxicology Research’, (2010), pp. 563–575. doi: 10.1039/c4tx00110a.

Franci, G. *et al.* (2015) ‘Silver nanoparticles as potential antibacterial agents’, *Molecules*, 20(5), pp. 8856–8874. doi: 10.3390/molecules20058856.

Hajipour, M. J. *et al.* (2012) ‘Antibacterial properties of nanoparticles’, *Trends in Biotechnology*. Elsevier Ltd, 30(10), pp. 499–511. doi: 10.1016/j.tibtech.2012.06.004.

Ivask, A. *et al.* (2013) ‘Toxicity of Ag , CuO and ZnO nanoparticles to selected environmentally relevant test organisms and mammalian cells in vitro : a critical review’, pp. 1181–1200. doi: 10.1007/s00204-013-1079-4.

Jung, W. K. *et al.* (2008) ‘Antibacterial Activity and Mechanism of Action of the Silver Ion in Staphylococcus aureus and Escherichia coli □’, 74(7), pp. 2171–2178. doi: 10.1128/AEM.02001-07.

Kar, S. *et al.* (2014) ‘Biochimica et Biophysica Acta Synthesis and characterization of Cu / Ag nanoparticle loaded mullite nanocomposite system : A potential candidate for antimicrobial and therapeutic applications’, *BBA - General Subjects*. Elsevier B.V., 1840(11), pp. 3264–3276. doi: 10.1016/j.bbagen.2014.05.012.

Khashan, K. S., Jabir, M. S. and Abdulameer, F. A. (2018) ‘Preparation and characterization

of copper oxide nanoparticles decorated carbon nanoparticles using laser ablation in liquid', *Journal of Physics: Conference Series*, 1003(1). doi: 10.1088/1742-6596/1003/1/012100.

Konieczny, J. and Rdzawski, Z. (2012) 'Antibacterial properties of copper and its alloys', *Archives of Materials Science and Engineering*, 56(7), pp. 53–60.

Kumar, A. *et al.* (2013) 'Facile synthesis of size-tunable copper and copper oxide nanoparticles using reverse microemulsions', *RSC Advances*, 3(15), p. 5015. doi: 10.1039/c3ra23455j.

Kumar, H. and Rani, R. (2013) 'Structural and Optical Characterization of ZnO Nanoparticles Synthesized by Microemulsion Route', *International Letters of Chemistry, Physics and Astronomy*, 19, pp. 26–36. doi: 10.18052/www.scipress.com/ilcpa.19.26.

Kumar, S. S. *et al.* (2013) 'Synthesis , characterization and optical properties of zinc oxide nanoparticles', pp. 1–6.

Millaty Abadiah, N. *et al.* (2019) 'Nanostructure, Band Gap, and Antibacterial Activity of Spinel Fe2MO4/OO Magnetic Fluids', *IOP Conference Series: Earth and Environmental Science*, 276(1). doi: 10.1088/1755-1315/276/1/012064.

Mondal, K. (2017) 'Recent Advances in the Synthesis of Metal Oxide Nanofibers and Their Environmental Remediation Applications', pp. 1–29. doi: 10.3390/inventions2020009.

Mugwang'a, F. K. *et al.* (2013) 'Optical characterization of Copper Oxide thin films prepared by reactive dc magnetron sputtering for solar cell applications', *International Journal of Thin Films Science and Technology*, 2(1), pp. 12–24. doi: 10.1016/S0042-207X(00)00151-2.

Nakata, K., Tsuchido, T. and Matsumura, Y. (2010) 'Antimicrobial cationic surfactant , cetyltrimethylammonium bromide , induces superoxide stress in Escherichia coli cells', pp. 568–579. doi: 10.1111/j.1365-2672.2010.04912.x.

Palza, H. (2015) 'Antimicrobial Polymers with Metal Nanoparticles', pp. 2099–2116. doi: 10.3390/ijms16012099.

Pandey, P. *et al.* (2014) 'Antimicrobial properties of CuO nanorods and multi-armed nanoparticles against B . anthracis vegetative cells and endospores', pp. 789–800. doi: 10.3762/bjnano.5.91.

Pandey, P. K. *et al.* (2014) 'Contamination of water resources by pathogenic bacteria', *AMB Express*, 4(1), pp. 1–16. doi: 10.1186/s13568-014-0051-x.

Periyat, P. and Ullattil, S. G. (2015) ‘Sol-gel derived nanocrystalline ZnO photoanode film for dye sensitized solar cells’, *Materials Science in Semiconductor Processing*. Elsevier, 31, pp. 139–146. doi: 10.1016/j.mssp.2014.11.022.

Reverberi, A. Pietro *et al.* (2016) ‘Synthesis of Copper Nanoparticles in Ethylene Glycol by Chemical Reduction with Vanadium (+ 2) Salts’, pp. 1–11. doi: 10.3390/ma9100809.

Roselina, N. R. N. and Azizan, A. (2012) ‘Ni nanoparticles : Study of particles formation and agglomeration’, 41, pp. 1620–1626. doi: 10.1016/j.proeng.2012.07.359.

Sahooli, M., Sabbaghi, S. and Saboori, R. (2012) ‘Synthesis and characterization of mono sized CuO nanoparticles’, *Materials Letters*. Elsevier B.V., 81, pp. 169–172. doi: 10.1016/j.matlet.2012.04.148.

Salas Orozco, M. F. *et al.* (2019) ‘Molecular mechanisms of bacterial resistance to metal and metal oxide nanoparticles’, *International Journal of Molecular Sciences*, 20(11). doi: 10.3390/ijms20112808.

Topnani, N., Kushwaha, S. and Athar, T. (2010) ‘Wet Synthesis of Copper Oxide Nanopowder’, *International Journal of Green Nanotechnology: Materials Science and Engineering*, 1(2). doi: 10.1080/19430840903430220.

Varughese, G., Jithin, P. and Usha, K. (2015) ‘Determination of Optical Band Gap Energy of Wurtzite ZnO: Ce Nanocrystallites’, *Physical Science International Journal*, 5(2), pp. 146–154. doi: 10.9734/psij/2015/14151.

Wang, Y. *et al.* (2016) ‘Electronic structures of C u2 O, C u4 O3, and CuO: A joint experimental and theoretical study’, *Physical Review B*, 94(24). doi: 10.1103/PhysRevB.94.245418.

Xiu, Z. *et al.* (2012) ‘Negligible Particle-Speci fi c Antibacterial Activity of Silver Nanoparticles’, pp. 10–14.

Zhang, J. (2011) ‘Silver-coated Zinc Oxide Nanoantibacterial Synthesis and Antibacterial Activity Characterization J .., V3-95’, (Iceoe), pp. 94–98.